Current Research (2020) Newfoundland and Labrador Department of Natural Resources
Geological Survey, Report 20-1, pages 29-48

MAJOR- AND TRACE-ELEMENT GEOCHEMISTRY OF MAFIC SILLS AND DYKES FROM THE NEW QUÉBEC OROGEN, WESTERN LABRADOR

J.P. Butler
Regional Geology Section

ABSTRACT

This report presents whole-rock major- and trace-element data of mafic sills and dykes from the New Québec Orogen of western Labrador. The data include samples from the Wakuach and Gerido intrusive suites (also known as the Montagnais Group), which previous geochronological studies indicate were emplaced into volcanosedimentary rocks of the Kaniapiskau Supergroup (KS) in two main stages, at ca. *2.17 and 1.88 Ga, respectively. In addition, data for amphibolite dykes from the nearby McKenzie River Domain (MRD) are included to test regional correlations between the MRD and the KS. Most of the samples are subophitic gabbronorites, although olivine- and quartz-bearing varieties, the latter with granophyric quartz–K-feldspar intergrowths, are found locally. The amphibolites are recrystallized, but based on field observations are interpreted as metamorphosed gabbroic dykes. The analyzed samples span a relatively broad compositional range, with magnesium numbers (Mg#) from 23–74. All samples, irrespective of group, are of tholeiitic basaltic composition. The gabbros exhibit decreasing Al_2O_3, CaO, Cr, and Ni, and increasing SiO_2, with increased fractionation (lower Mg#), consistent with the fractionation of plagioclase, olivine, clinopyroxene, and orthopyroxene. Rare-earth element (REE) and extended trace-element patterns are mid-ocean ridge basalt (MORB)-like, with overall flat patterns ($(La/Yb)_{CN}$= 0.63–2), negligible Eu anomalies (Eu/Eu*= 0.73–1.28), and variable, but generally low, $(Th/Nb)_{CN}$ (0.34–7.06), indicative of relatively minor crustal contamination during ascent. The presented data are consistent with previous tectonic interpretations that sill emplacement was the result of lithospheric-scale rifting of the eastern Superior margin. Geochemical similarities suggest the MRD dykes may be co-magmatic with either of the Wakuach–Gerido intrusive suites, although at present, the timing of mafic magmatism in the MRD is not known.*

INTRODUCTION

The Paleoproterozoic volcanosedimentary successions underlying the New Québec Orogen (NQO) of western Labrador are intruded by two generations of mafic to locally ultramafic sills, historically referred to as the Montagnais Group or Montagnais Sills (Baragar, 1960; Wardle and Bailey, 1981; T. Krogh and B. Dressler, cited by Clark, 1984; Findlay *et al.*, 1995; Findlay, 1996). The sills are mostly found in allochthonous zones in the central part of the orogen, where they form several-km-thick complexes intruded into the surrounding metasedimentary and metavolcanic rocks of the Kaniapiskau Supergroup (KS; Baragar, 1960; Findlay, 1996). Elsewhere in the orogen they are known to locally host base-metal, precious-metal and platinum-group-element (PGE) mineralization (*e.g.*, *see* Lacroix and Darling, 1991; Smith *et al.*, 2018, Conliffe *et al.*, 2019), and represent an important exploration target in western Labrador. In addition, the sills are of general scientific interest as potential indicators of the lithospheric-scale evolution of the Superior margin prior to *ca.* 1.8 Ga Hudsonian orogeny.

This report describes and interprets the whole-rock major- and trace-element geochemistry of mafic sills from the central NQO in western Labrador, spanning NTS map areas 23I/12 (Andre Lake), 23I/13 (Marion Lake) and 23J/16 (Hollinger Lake). The data comprise 71 samples collected in 2017 and 2018 as part of regional mapping program conducted by GSNL, and are available online to the public in two Open File data releases (Butler, 2019a, b). The report starts with a brief review of the regional geology of the NQO in western Labrador, followed by a summary of the distribution and lithological features of the sills, and their basic petrography. The geochemical data are presented in the form of classification and multi-element diagrams, with an emphasis on comparing samples from different lithotectonic domains. Finally, the data are discussed in the context of previous work and tectonic models for the evolution of the Superior margin.

REGIONAL GEOLOGY OF THE NQO IN WESTERN LABRADOR

The NQO (historically the Labrador Trough) is a north–south-trending orogenic belt extending ~1600 km from Ungava Bay southward through northern Québec and western Labrador (Figure 1; Hoffman, 1988). It represents the southeastern arm of the much larger *ca.* 1.8 Ga Trans-Hudson orogen, formed when the eastern margin of the Superior Craton collided with the Core Zone, an assemblage of Archean crustal blocks (Wardle *et al.*, 2002; Corrigan *et al.*, 2018), following closure of the Manikewan Ocean (Wardle *et al.*, 2002; Corrigan *et al.*, 2009). Collision resulted in the formation of a west-vergent fold-and-thrust belt built from supracrustal rocks deposited along the eastern margin of the Superior Craton, and to the east more distal and suspect domains (Wares and Goutier, 1990; Wardle *et al.*, 2002). In the eastern hinterland of the orogen, high-grade metamorphism accompanied the formation of large-scale basement-cored nappes and anticlines (Moorhead and Hynes, 1990).

This report assesses the central part of the NQO in western Labrador, where the mostly sub- to greenschist-facies volcanosedimentary rocks of the KS and associated intrusions are deformed into orogen-parallel folds cut by east- to northeast-dipping thrust faults (Figure 2; Wardle, 1982). The KS in western Labrador is subdivided into three stratigraphic cycles bounded by erosional unconformities (Figure 3; Wardle and Bailey, 1981; Clark and Wares, 2005). The first cycle was deposited unconformably on Archean Superior basement, and comprises conglomerates and sandstones (Seward Group), locally associated with alkaline basalts–andesites, overlain by turbidites and interlayered tholeiitic basalts (Le Fer Formation), and finally shallow-water carbonates (Denault Formation dolomites) and siltstones (Dolly Formation; Wardle and Bailey, 1981). This cycle is interpreted to reflect initial rifting and later subsi-

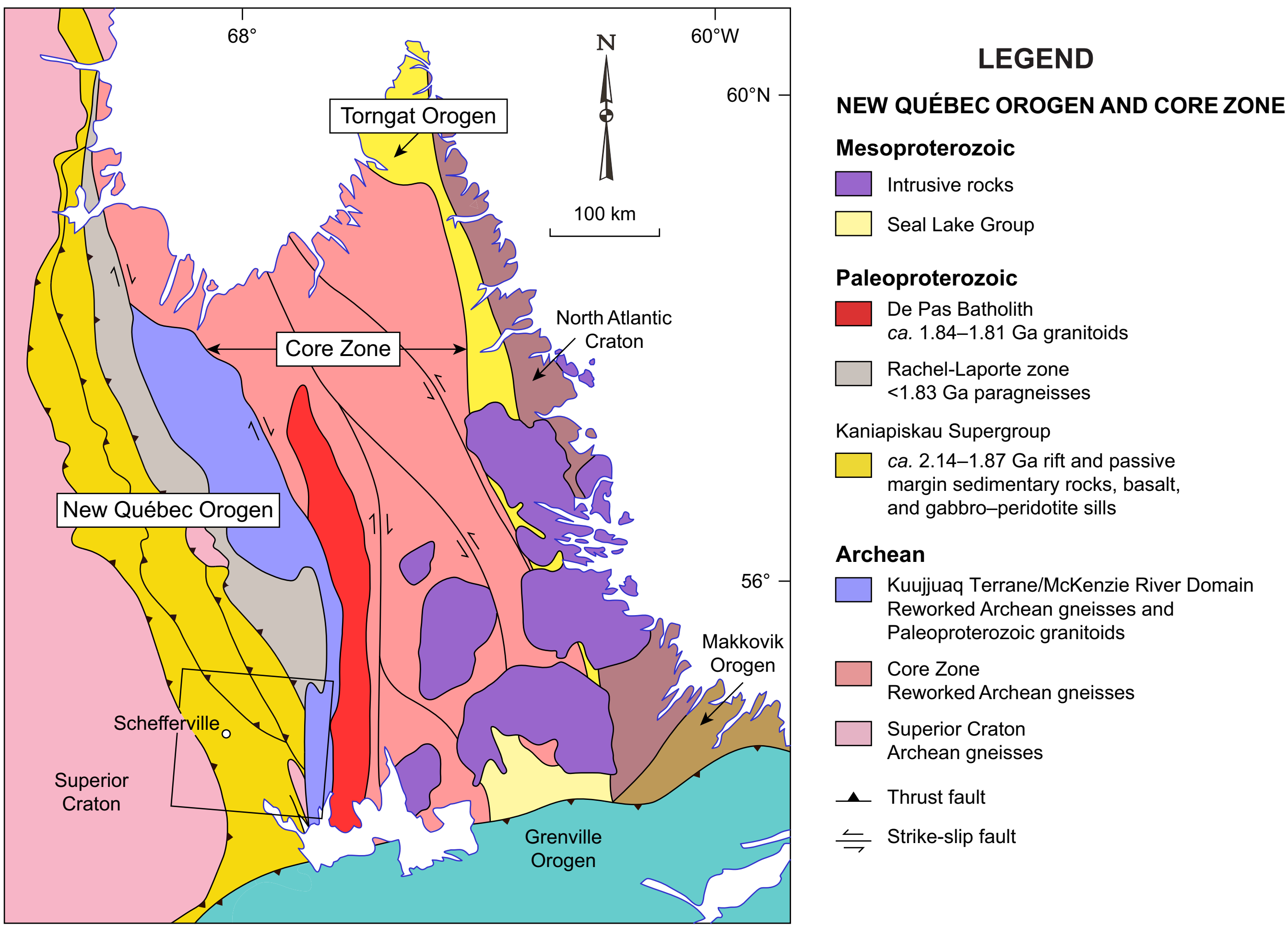

Figure 1. *Simplified geological map highlighting the main tectonic elements of Labrador. The NQO is a north–south-trending orogenic belt that records collision between the Superior craton and the Core Zone at* ca. *1.8 Ga. Box shows approximate extent of Figure 2.*

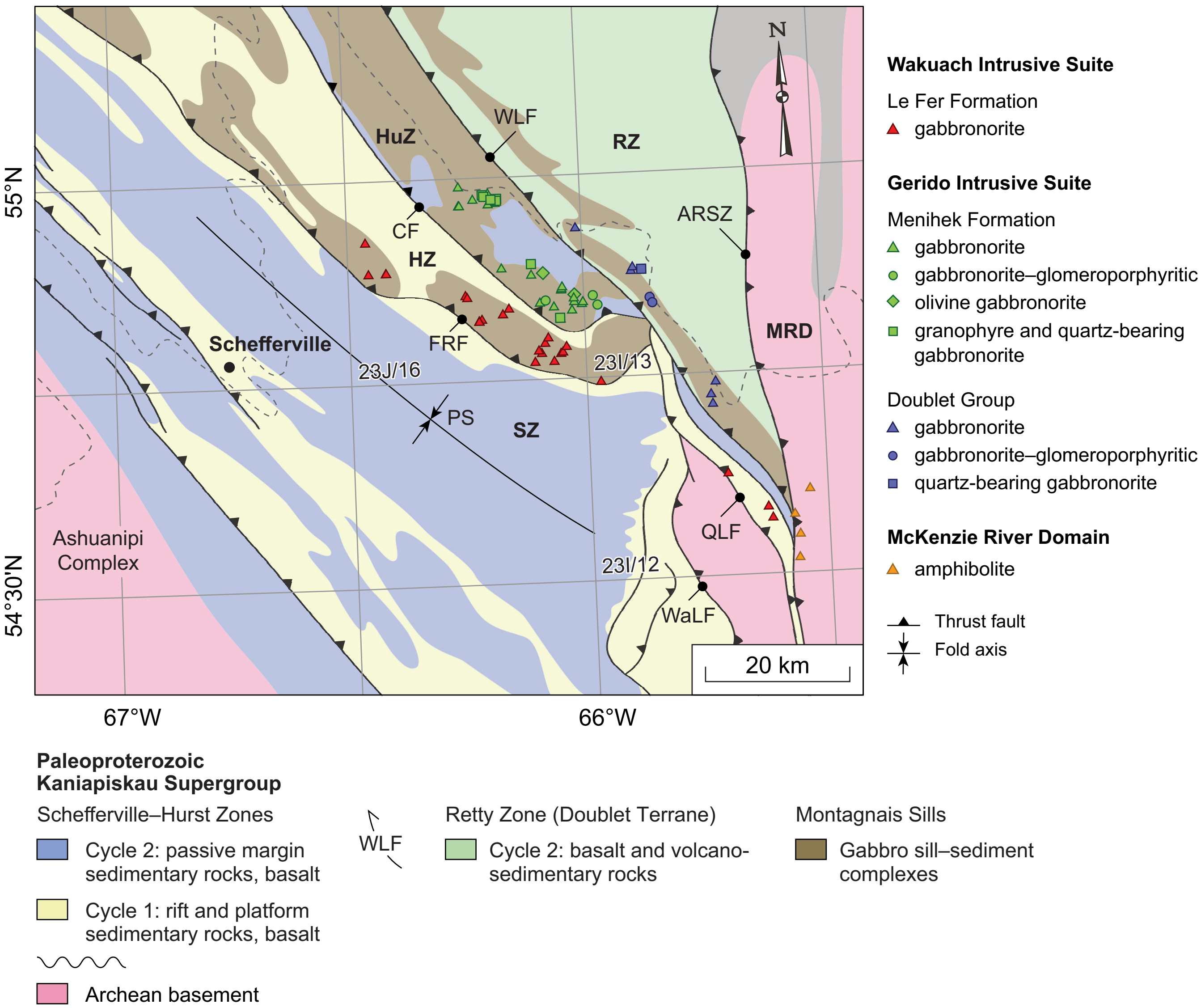

Figure 2. *Simplified geological map of the central NQO in western Labrador, showing sample locations coloured according to the formation they intrude, and their lithological type (*see *text for details). Thrust faults separate the orogen into a series of tectonic zones, including the Schefferville Zone (SZ), the Howse Zone (HZ), the Hurst Zone (HuZ), and the Retty Zone (RZ). Thrust faults include the Ferrum River Fault (FRF), the Chassin Fault (CF), the Walsh Lake Fault (WLF), the Wade Lake Fault (WaLF), and the Quartzite Lake Fault (QLF). The Ashuanipi River Shear Zone (ARSZ), a dextral-transpressive shear zone, separates the low-grade rocks of the Kaniapiskau Supergroup from reworked Archean orthogneisses of the McKenzie River Domain (MRD). Map grid lines (solid grey) denote 1:50 000-scale NTS map areas (Hollinger Lake, 23J/16; Marion Lake, 23I/13; Andre Lake, 23I/12). The studied areas lie to the north and east of the southeast-trending, regional-scale Petitsikapau Synclinorium (PS).*

dence–marine transgression along the present-day eastern margin of the Superior Craton (Wardle and Bailey, 1981; Findlay, 1996). Equivalent successions found along the northern and western peripheries of the eastern Superior Craton suggest this was part of a widespread–plate-scale tectonic event (St-Onge *et al.*, 2000), perhaps related to the opening of an ocean basin (the Manikewan Ocean; Stauffer, 1984).

The second cycle (Ferriman Group) comprises a transgressive sequence including sandstones (Wishart Formation), black shale (Ruth Formation), iron formation (Sokoman Formation), and sub-alkaline to alkaline basalts (Nimish Formation) overlain by a thick succession of turbidites and associated tholeiitic basalts (Menihek Formation; Figure 3; Wardle and Bailey, 1981, 1982; Clark and Wares, 2005). To the east, the Ferriman Group is in fault

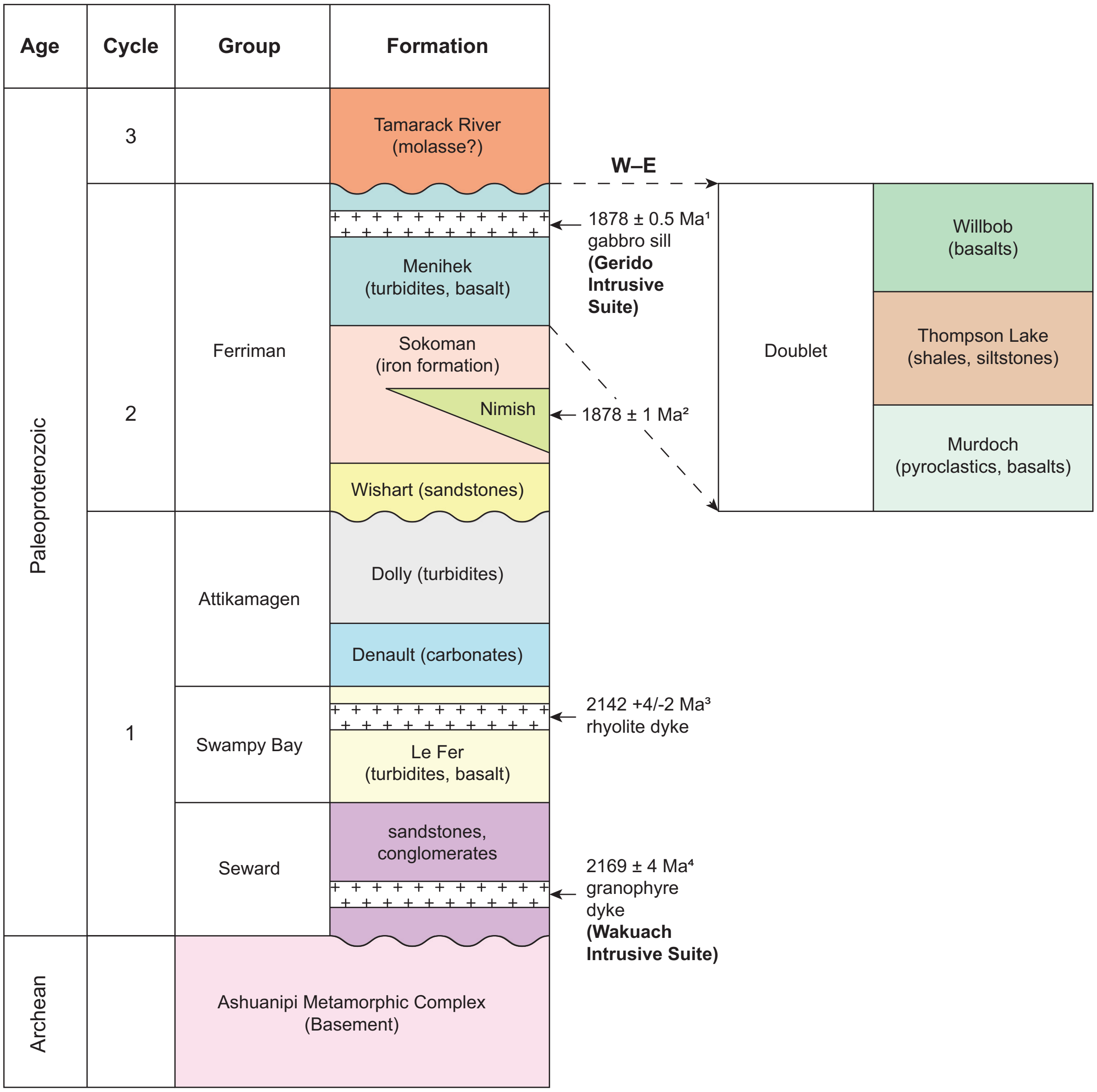

Figure 3. *Generalized stratigraphic column showing the main sedimentary units of the KS in western Labrador (from Butler, 2019c). The Doublet Group is considered to be correlative with the Cycle 2 Ferriman Group. Geochronological data (with superscripts) from: (1) Bleeker and Kamo (2018); (2) Findlay* et al. *(1996); (3) T. Krogh and B. Dressler, cited by Clark (1984); (4) Rohon* et al. *(1993).*

contact (along the Walsh Lake Fault) with mafic volcanoclastic rocks (Murdoch Formation), shales–siltstones (Thompson Lake Formation), and tholeiitic basalts (Willbob Formation) of the Doublet Group, considered its distal, deeper water correlative based on limited geochronological data (*e.g.*, Findlay *et al.*, 1995). Tectonic models for second cycle sedimentation and volcanism range from a foredeep setting (Hoffman, 1987), to an embryonic oceanic rift analogous to the Gulf of California (Wardle and Bailey, 1981; Skulski *et al.*, 1993).

The third cycle comprises arkosic sandstones of the Tamarack River Formation (Clark and Wares, 2005), interpreted as syn-orogenic molasse. Cycle 3 rocks have not been identified in the study area (Figure 2).

Cycles 1 and 2 of the KS are each intruded by several-km-thick complexes of tholeiitic gabbro (and locally peridotite) sills, which form the basis of the present study. The distribution and lithology of the sills are described in the following section. The sills have been historically combined into one group, referred to by many names, including the

Montagnais Intrusives (Frarey and Duffell, 1964), and Montagnais Group (Baragar, 1967). More recently, Bilodeau and Caron-Côté (2018) introduced the term Wakuach Intrusive Suite to refer to all sills intruding the first cycle, whereas those intruding the second cycle are termed the Gerido Intrusive Suite. This report adopts these terms, but further subdivides the gabbros according to the formations–groups they intrude (following Findlay, 1996) to facilitate regional comparison.

The available geochronological data, although limited, suggest that the Wakauch and Gerido intrusive suites were emplaced in two separate stages, at *ca.* 2.17 and *ca.* 1.88 Ga, respectively, corresponding to important changes in sedimentation along the Superior margin. Wakuach Intrusive Suite gabbros were emplaced 2169 ± 4 Ma (Figure 3; Rohon *et al.*, 1993), the age of a gabbro sill intruding the Chakonipau Formation (Seward Group) at the base of Cycle 1. Rifting and deposition of Cycle 1 conglomerates–sandstones were therefore underway by *ca.* 2.17 Ga. Subsequent Cycle 1 marine transgression and passive margin sedimentation took place before 2142 +4/-2 Ma, the age of a rhyolite dyke cutting the upper Bacchus Formation basalts, which are correlative with the Le Fer Formation (Figure 3; Swampy Bay Group) in the present study area (T. Krogh and B. Dressler, *in* Clark, 1984).

Later emplacement of the Gerido Intrusive Suite took place by 1878 ± 0.5 Ma, the age of a gabbro sill that cuts the Menihek Formation at Howse Lake (Findlay *et al.*, 1995; Bleeker and Kamo, 2018), and continued until at least 1874 ± 3, the age of a gabbro sill intruding into basalts of the Hellancourt Formation (Machado *et al.*, 1997), correlative with the Ferriman Group (Clark and Wares, 2005) in the northern part of the orogen.

At the eastern edge of the NQO in Labrador, the Ashuanipi River Shear Zone (ARSZ) marks the boundary between the KS and reworked Archean orthogneisses of the McKenzie River Domain (MRD; James and Dunning, 2000). Protolith ages of 2776 ± 5 Ma from orthogneisses underlying the MRD suggest it is of Superior affinity (James and Dunning, 2000), although its precise history, which may have included rifting and separation from the Superior margin prior to Hudsonian collision remains speculative. Amphibolite boudins and layers are common in the MRD orthogneisses, and probably represent deformed equivalents of mafic dykes observed by Wardle (1979) near Lac Verrazano in the Marion Lake area. Wardle and Bailey (1981) speculated that the latter represent feeder dykes related to sills intruded into the KS, based on similarities in their major-element compositions, although no trace-element data were obtained. Four samples of MRD amphibolites have been included here to test this hypothesis.

REGIONAL DISTRIBUTION AND LITHOLOGICAL CHARACTERISTICS OF MAFIC SILLS AND DYKES

The analyzed samples were collected in 2017 and 2018 during regional mapping of NTS map areas 23I/12 (Andre Lake), 23I/13 (Marion Lake) and 23J/16 (Hollinger Lake), in the eastern part of the NQO of western Labrador (Figure 2). The bedrock geology can be divided into structurally allochthonous zones separated by northwest–southeast- to north–south-trending thrust faults formed during Hudsonian collision. The distribution of sills in these zones, and their first-order characteristics, are summarized below. Note that parts of the region, particularly the Hollinger Lake area, are characterized by exceptionally poor bedrock exposure. Some of the features described below are therefore based on the observations of Findlay (1996), who provided a detailed examination of sills near Howse Lake area, ~40 km along-strike of the Hollinger Lake area.

WAKUACH INTRUSIVE SUITE

The Wakuach Intrusive Suite gabbros include all gabbro sills intruded into Cycle 1 rocks. In this study, they are represented by the Le Fer gabbros of the Howse Zone, which trends northwest–southeast through the Hollinger Lake area, and by gabbros intruded into Cycle 1 rocks in the Andre Lake area, and included by Clark and Wares (2005) in the Schefferville Zone.

The Howse Zone lies between the Ferrum River Fault (FRF), which cuts the northern limb of the regional-scale Petitsikapau Synclinorium, and the Chassin Fault (CF, Figure 2). The zone is primarily underlain by Cycle 1 shales and basalts (Le Fer Formation), in addition to sandstones (Seward Group). Gabbro sills, forming ~5-km-thick complexes with interlayered basalt and shales, are exposed in two anticlines adjacent to the Ferrum River Fault. Individual sill thicknesses were not measured, but in the section near Howse Lake range from ~50–600 m (Findlay, 1996). In the Hollinger Lake (NTS 23J/16) area, most of the Le Fer gabbros comprise dark-grey, aphyric to medium-grained equigranular gabbro (Plate 1A). Networks of anastomosing felsic veins cut some outcrops (Plate 1B), in addition to late quartz veins. Contacts with adjacent sedimentary rocks exhibit aphanitic margins, and the sedimentary units are typically gossanous.

The Andre Lake area (Figure 2; NTS 23I/12) is situated to the southeast of the Hollinger Lake area, and is structurally unique in this part of the orogen, comprising a central, basement-cored anticline flanked by rocks of Cycles 1 and 2. In this area, the southeast-trending faults defining the

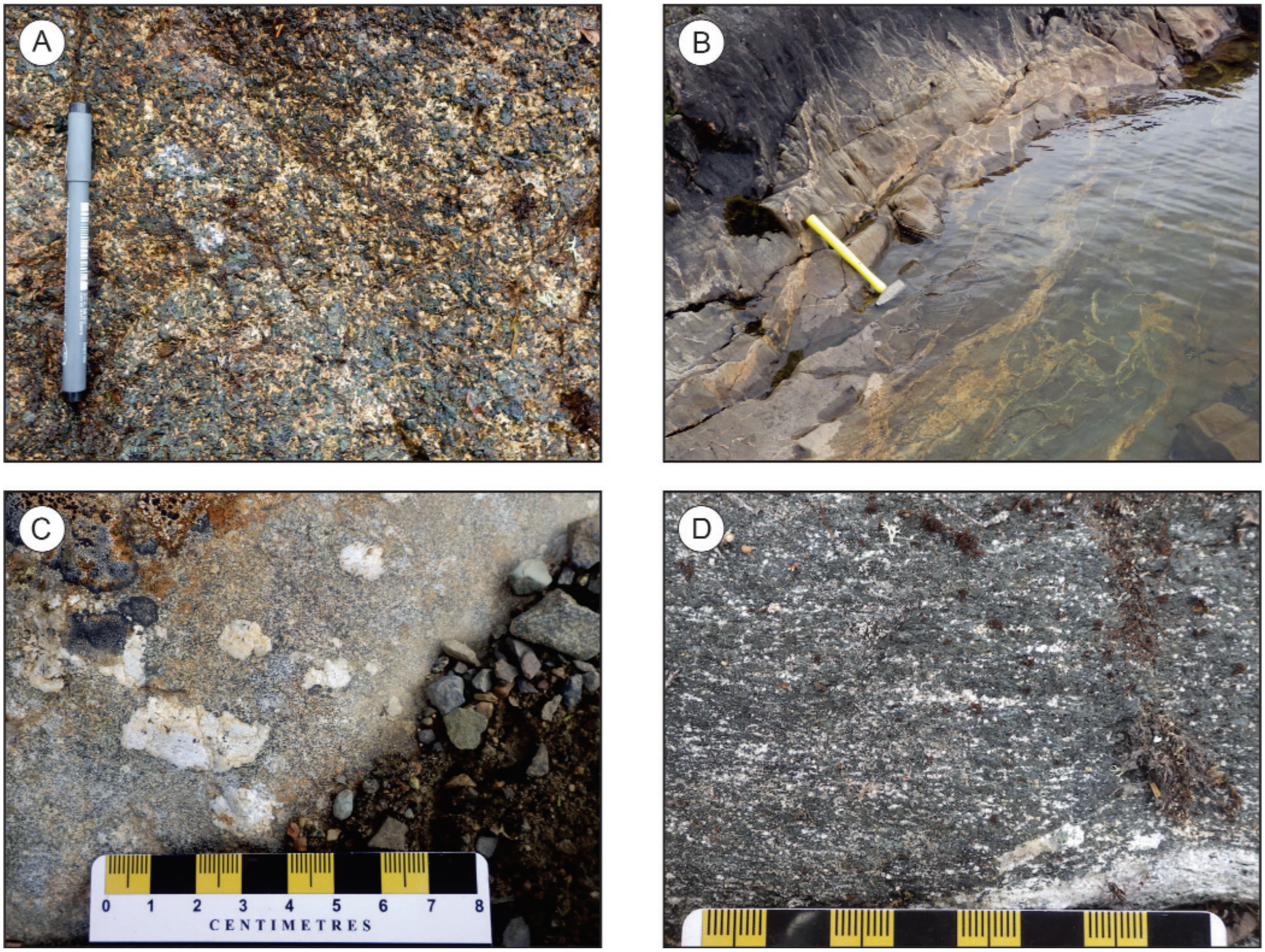

Plate 1. *Photographs showing field aspects of gabbros and amphibolites from the study area. A) Medium-grained magnetite-bearing Le Fer Gabbro from the Howse Zone, Hollinger Lake area; B) Felsic veins cutting Le Fer Gabbro in the Hollinger Lake area; C) Glomeroporphyritic Menihek Gabbro from the Hurst Zone; D) Medium-grained, foliated amphibolite lens from the McKenzie River Domain.*

Howse and other zones north of the Petitsikapau Synclinorium swing into southward orientations parallel to the ARSZ. Most of the Andre Lake area is shown by Clark and Wares (2005) to be part of the Schefferville Zone, which encompasses the foreland of the orogen and is largely underlain by Cycle 2 turbidites (Menihek Formation) and iron formation. This subdivision may require revision, given that the Andre Lake anticline is such a distinct structural feature, and that the flanking sedimentary units and associated gabbros are similar to, albeit stratigraphically much thinner than, those in the Howse and Hurst zones. In following sections, gabbros intruded into Cycle 1 rocks on the flanks of the Andre Lake anticline have been included with those from zones north of the Petitsikapau Synclinorium according to the units they intrude as described below.

The Wakuach Intrusive Suite is represented in the Andre Lake area by gabbro sills intruded into the Seward Group sandstones and Le Fer Formation phyllites on both the eastern and western limbs of the Andre Lake anticline. The sills there are thin by comparison with the thick complexes seen in the Howse Zone, typically a few hundred metres, but are lithologically similar, comprising dark-grey, aphyric to medium-grained equigranular gabbro. Metamorphic grade is higher in the Andre Lake area, however, particularly on the eastern limb of the anticline, where gabbro sills exhibit amphibolitized margins with strong lineations likely related to dextral transpression along the ARSZ.

GERIDO INTRUSIVE SUITE

The Gerido Intrusive Suite refers to all mafic–ultramafic sills intruded into Cycle 2 rocks, and includes the

Menihek gabbros and the Doublet gabbros of the Hurst and Retty zones, respectively.

The Menihek gabbros are exposed in the Hurst Zone, a northeast-facing succession of Menihek Formation shales intruded by a ~10-km-thick pile of aphyric to plagioclase–glomeroporphyritic gabbro sills with interlayered basalts and sedimentary rocks, situated north of the Chassin Fault. Findlay (1996) showed that some Menihek sills near Howse Lake exhibit a distinct stratification consisting of narrow chilled margins, an upper and lower gabbroic phase consisting of aphyric to sparsely glomeroporphyritic dark-grey gabbro, and a middle zone of coarser grained, highly glomeroporphyritic (30–50% glomerocrysts) gabbro–anorthosite. In addition, in the upper parts of some sills, the gabbroic phase grades into felsic zones that form irregular lenses and pods (locally pegmatitic), ranging in composition from quartz gabbro to granite (Findlay, 1996). The Menihek gabbros in the Hollinger Lake area exhibit features similar to those reported by Findlay (1996). Most outcrops comprise dark-grey, aphyric to medium-grained equigranular gabbro. Glomeroporphyritic varieties are found locally (Plate 1C), although they generally comprise relatively few glomerocrysts (<10%). No outcrops resembling the anorthositic internal zones documented by Findlay (1996) were observed in the Hollinger Lake area, although this may be due to poor exposure.

North of the Walsh Lake Fault, in the Retty Zone, the Doublet gabbros intrude into a comparatively narrow belt of shales (Thompson Lake Formation), situated beneath a thick succession of basalt (Willbob Formation). As noted above, the rocks of the Doublet Group are interpreted to represent deeper water correlatives of the Cycle 2 Ferriman Group (Findlay *et al.*, 1995). Samples from the Retty Zone were collected in all three map areas studied here. Like the Menihek gabbros, the Doublet gabbros are mostly aphyric to sparsely glomeroporphyritic (<10% glomerocrysts). Associated ultramafic rocks, unique to sills in the Retty Zone, include peridotite, pyroxenite, and serpentinite. Some of these units represent parts of differentiated mafic–ultramafic sills (Lacroix and Darling, 1991), whereas others show intrusive contacts with adjacent gabbros (Bilodeau and Caron-Côté, 2018). Ultramafic rocks in the Labrador segment of the NQO are restricted to a narrow slice adjacent to the border in the northern part of the Marion Lake area. One sample was collected for geochemical analysis, but has been excluded from this report pending further mapping and sampling.

McKENZIE RIVER DOMAIN AMPHIBOLITES

East of the ARSZ, the orthogneisses of the MRD contain abundant, deformed amphibolite lenses interpreted as deformed dykes, possibly related to the Montagnais Sills (Wardle and Bailey, 1981), although their age is not known. These bodies range in thickness from ~10–100 m thick, and are typically deformed into concordance with the dominant north–south fabric in the MRD. A few outcrops exhibit relict gabbroic textures, but most have been completely transformed to fine- to medium-grained weakly foliated amphibolite (Plate 1D), typically with biotite-rich margins. Within the ARSZ, the dykes have been mylonitized along with the surrounding orthogneiss. Samples have been included in this study to examine possible correlations with the Wakuach Suite and Gerido intrusive suites.

PETROGRAPHIC OBSERVATIONS

The studied gabbros are divided into three types based on their inferred primary mineralogical and textural features. The majority of the samples (from all groups) are fine- to medium-grained, subophitic- to ophitic-textured gabbronorites, consisting of plagioclase, clinopyroxene, and subordinate orthopyroxene, in addition to minor Fe–Ti oxides (Plate 2A). Minor primary hornblende appears in some samples. Compositionally and texturally, these samples appear similar to the homogeneous aphyric sills and the gabbroic phases of layered sills described by Findlay (1996). All of the samples have undergone some degree of alteration and/or metamorphism, manifested in the partial replacement of pyroxenes by fine-grained aggregates of chlorite, prehnite, and pumpellyite. Actinolite is common in sills from the Andre Lake area, where metamorphic grade was higher, and in some instances, deformed sill margins have been completely transformed to actinolite schist.

Glomeroporphyritic textures, with clusters of sericitized plagioclase phenocrysts, are present among samples of Menihek and Doublet gabbros. Mineralogically, the glomeroporphyritic samples are also gabbronorites, and typically exhibit a fine-grained subophitic matrix comprising plagioclase, clinopyroxene, and orthopyroxene, surrounding glomerocrysts that range in size from <1–5 cm in diameter. As noted above, the present samples are only sparsely glomeroporphyritic (<10% glomerocrysts).

A few of the Menihek samples contain up to ~10% relict olivine (Plate 2B). Olivine in these samples forms irregular, rounded grains, possibly the result of resorption, included in clinopyroxene and orthopyroxene oikocrysts. Unlike the pyroxenes, olivine lacks plagioclase inclusions, and is interpreted as an early phase. Most relict olivine grains are completely replaced by aggregates of fine-grained mica, likely talc. These olivine-bearing samples probably correspond to the olivine gabbronorites documented by Findlay (1996) in the central parts of some Menihek Gabbro sills.

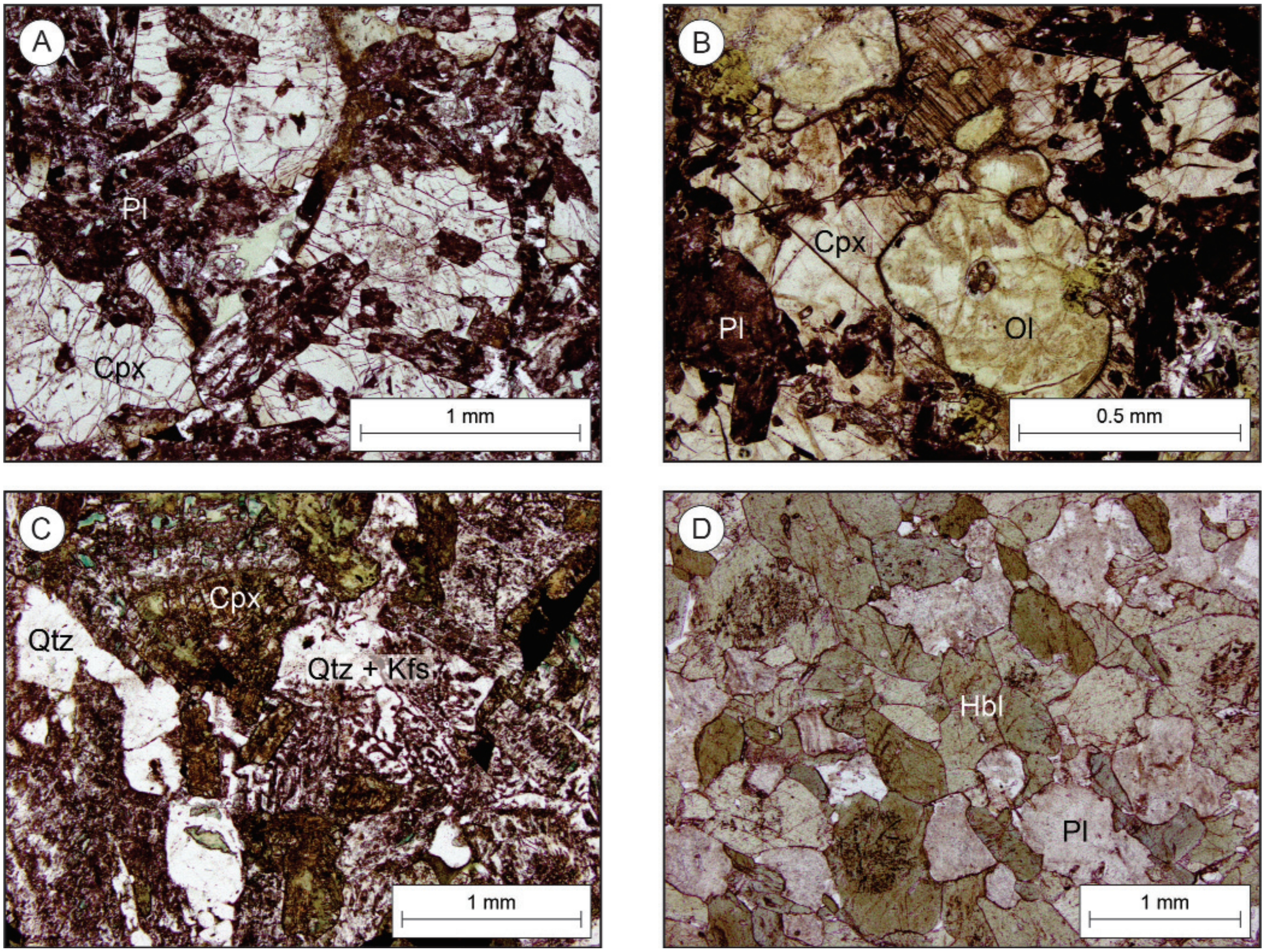

Plate 2. *Thin section photos showing representative petrographic features of the gabbro samples. A) Subophitic gabbro showing clinopyroxene with inclusions of dusty plagioclase (Le Fer Gabbro); B) Rounded (resorbed?) olivine grains partly included in clinopyroxene (Menihek Gabbro); C) Granophyric quartz–K-feldspar intergrowths in quartz-bearing gabbronorite (Menihek Gabbro); D) Amphibolite with granoblastic hornblende and plagioclase (MRD amphibolite). Key: Cpx–clinopyroxene, Pl–plagioclase, Ol–olivine, Qtz–quartz, Kfs–K-feldspar, Hbl–hornblende.*

A small number of Menihek Gabbro samples, and one Doublet Gabbro sample, are quartz-bearing gabbronorites. The Menihek samples are mineralogically and texturally similar to the other gabbronorites, but contain cm-scale patchy zones in which quartz and inferred alkali-feldspar form complex granophyric intergrowths (Plate 2C). These features were not recognized in the field, and so their context is somewhat unclear, but similar granophyric textures were described by Findlay (1996) from the upper "felsic zones" of stratified Menihek sills near Howse Lake.

The MRD amphibolites examined here are remarkably consistent in their mineralogy and texture. The least deformed samples comprise medium-grained granoblastic hornblende and plagioclase (Plate 2D). Some samples exhibit a weak foliation defined by the alignment of hornblende and thin, plagioclase-rich layers. Relict gabbroic textures were not observed in the studied thin sections, but have been reported elsewhere (Wardle, 1981).

METHODS

Data are presented for 23 samples representing the Wakuach Intrusive Suite (Le Fer gabbros), 42 samples representing the Gerido Intrusive Suite (34 Menihek gabbros and 8 Doublet gabbros), and 4 MRD amphibolites. The data are coloured according to these groups, and different symbols are assigned corresponding to the mineralogical–petrographic types noted above. Whole-rock major- and trace-element compositions were determined at the GSNL geochemistry laboratory following the analytical methods outlined by Finch *et al.* (2018). Major-element concentrations (in addition to Cr, Zr, Be, Sc and Ba) were analyzed by Inductively Coupled Plasma-Optical Emission Spectrometry (ICP-OES) following borate fusion. Ferrous iron (FeO) was calculated following the method of Wilson (1960). Volatiles were determined by loss-on-ignition at 1000°C. Rare-earth elements (REE) and selected trace elements were determined by Inductively Coupled Plasma-Mass Spectrometry (ICP-MS) following the same sample digestion procedure. Additional trace elements (As, Cd, Co, Cu, Li, Ni, Pb, Rb, V, Zn) were analyzed by ICP-MS following total-acid digestion.

GEOCHEMISTRY RESULTS

ALTERATION AND ELEMENT MOBILITY

Proper classification and petrogenetic interpretation of igneous rocks require separating their primary igneous geochemical features from those imparted during later metamorphism and/or hydrothermal alteration. In general, most major elements and the low-field-strength elements (LFSE; *e.g.*, Cs, Rb, K) are regarded as mobile during metamorphism and hydrothermal alteration, whereas select major elements (namely Al, Ti and P), high-field-strength elements (HFSE; *e.g.*, Y, Th, Nb), rare-earth elements (REE; except Ce, Eu), and transition metals (*e.g.*, Cr, Ni, Co) are considered relatively immobile and are thought to remain unaffected during postmagmatic processes (*e.g.*, Ludden *et al.*, 1982).

Figure 4 shows the degree of alteration of the analyzed samples using the Spitz and Darling (1978) index (wt. % Al_2O_3/Na_2O) plotted against wt. % Na_2O. Several of the samples contain less than 2 wt. % Na_2O, and there is a general increase in Al_2O_3/Na_2O with decreasing Na_2O, suggesting these samples have undergone Na-loss and residual gain in Al related to breakdown of sodic plagioclase, consistent with thin-section observations. Moreover, certain major elements, namely Na_2O, K_2O, and to a lesser extent CaO and SiO_2, show considerable scatter on bivariate plots (Figure 5; *see* below), further indicating that these elements underwent postmagmatic remobilization. Consequently, the classifications and petrogenetic interpretations presented below are based on the major and trace elements that show the least mobility during postmagmatic processes. With some exceptions (*see* below) all samples are shown on subsequent diagrams, regardless of their degree of alteration.

MAJOR- AND SELECTED TRACE-ELEMEMT CHEMISTRY

Major- and trace-element compositions of representative gabbro analyses for each group–lithological variety are provided in Table 1. All analyses can be found in Butler (2019a, b). On the whole, the gabbros contain moderate SiO_2 (43.81–53.66 wt. %), low to moderate MgO (2.66–13.17 wt. %) and moderate to high FeO_T (=FeO+0.9*Fe_2O_3) (6.90–18.01 wt. %), corresponding to Mg#s of 23–74, where Mg# = mol. Mg/(Mg+FeO_T)*100. The lowest Mg#s, corresponding to the most evolved samples, are found among the quartz-bearing Menihek gabbros. TiO_2 ranges from 0.50–3.14 wt. %, with higher values corresponding to glomeroporphyritic Menihek and Doublet gabbronorites, and quartz-bearing Menihek gabbros. Al_2O_3 is variable (10.85–21.38 wt. %), with the highest values found among the aphyric and glomeroporphyritic Menihek gabbros. Loss on ignition (LOI) values range from 0.65–3.8 wt. % among the presented samples, consistent with the widespread presence of hydrous secondary minerals noted above.

Figure 5 shows selected major-element concentrations plotted against Mg# as the index of differentiation, where lower Mg# represents more evolved compositions. Several first-order trends are apparent. The samples generally exhibit decreasing Al_2O_3 and CaO with increasing fractionation (lower Mg#). SiO_2, TiO_2 and P_2O_5, meanwhile, increase with fractionation. These trends are well illustrated by the Le Fer gabbros, which range from Mg#=39–67. The Menihek gab-

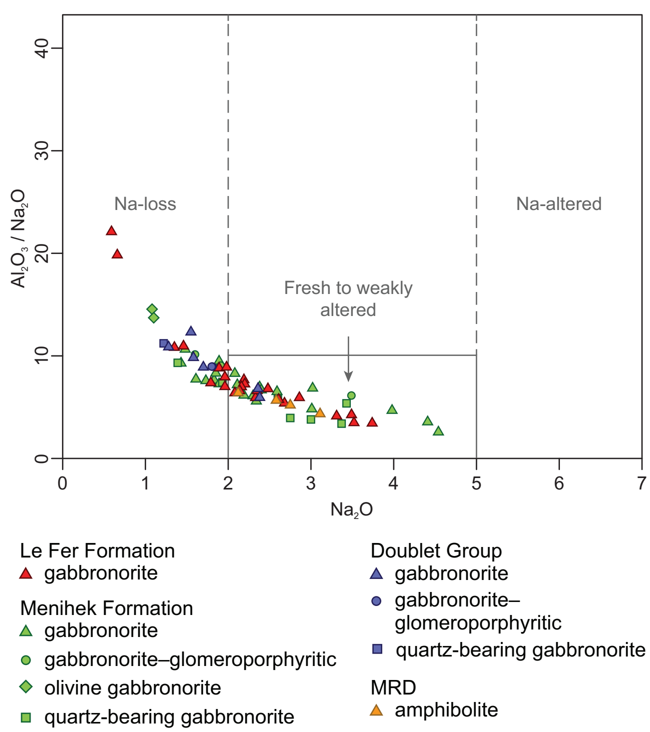

Figure 4. *Na_2O* vs. *Al_2O_3/Na_2O diagram (Spitz and Darling, 1978) showing the degree of sample alteration. Numerous samples plot below the "fresh to weakly altered" range of Na_2O values, and exhibit increasing Al_2O_3/Na_2O with decreasing Na_2O, suggesting Na-loss resulting from alteration of plagioclase.*

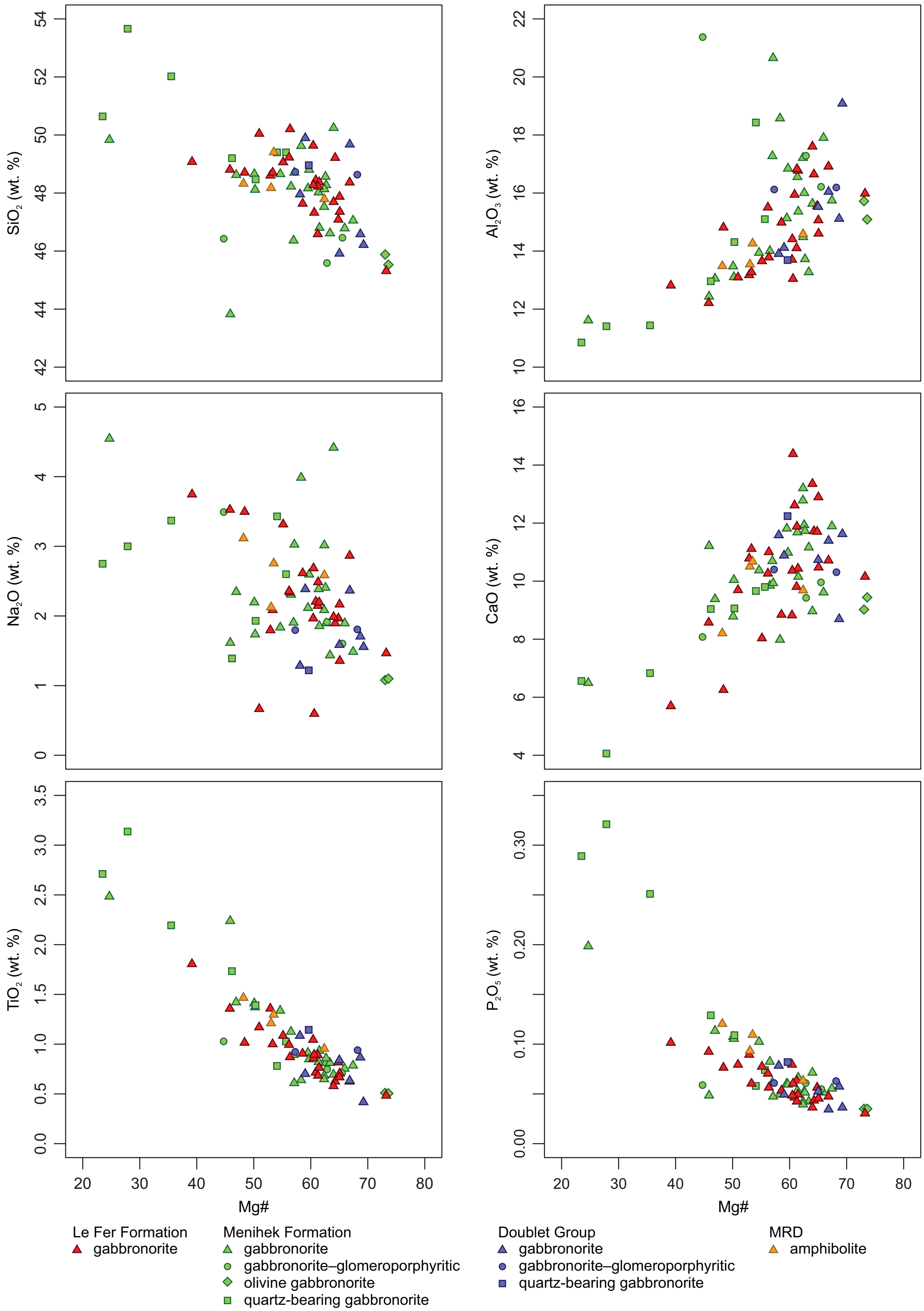

Figure 5. *Bivariate major-element diagrams showing selected major elements plotted against Mg# (*see *text).*

Table 1. Representative whole-rock geochemical data for the different gabbro groups (Le Fer, Menihek, Doublet) and MRD amphibolites. All data are available in Butler (2019a, b)

Sample	17JPB258A01	17JPB250A01	17JPB191A01	17JPB061A01	17JPB015A01	17JPB074A01	17JPB044A01	18JPB023A01
Group	Doublet	Doublet	Le Fer	Menihek	Menihek	Menihek	Menihek	MRD
Lithology		glom*		glom	olivine	quartz	amphibolite	
SiO_2	47.94	48.73	48.35	48.26	46.43	45.88	50.64	48.16
TiO_2	1.08	0.923	0.621	0.854	1.027	0.509	2.711	1.207
Al_2O_3	13.89	16.13	16.9	13.71	21.38	15.72	10.85	13.53
FeO	9.53	9.11	7.12	9.03	7.16	8.1	15.46	10.91
Fe_2O_3	2.36	1.82	1.7	0.89	1.22	1.27	2.01	1.91
MnO	0.218	0.188	0.162	0.216	0.179	0.147	0.326	0.219
MgO	7.41	6.85	8.04	8.51	3.25	12.31	2.66	6.91
CaO	11.57	10.4	10.7	11.72	8.07	9.02	6.56	10.49
Na_2O	1.28	1.8	2.86	1.89	3.49	1.08	2.75	2.12
K_2O	0.08	0.1	0.09	0.77	1.63	0.28	0.6	0.46
P_2O_5	0.078	0.061	0.047	0.051	0.059	0.035	0.289	0.093
LOI	2.15	2.52	2.73	2.32	3.47	3.62	1.81	0.89
Cr	173	287	456	555	24	130	3	169
Ni	86	93	99	114	30	295	17	79
Co	51	47	45	59	26	83	34	56
Sc	44.1	39	39.4	51.4	24	21.8	47.2	45.2
V	329	278	211	295	255	155	22	359
Cu	132	83	92	202	20	140	3	150
Pb	b.d.	b.d.	b.d.	15	2	b.d.	b.d.	b.d.
Zn	87	90	161	291	95	67	72	105
Mo	b.d.	b.d.	b.d.	b.d.	b.d.	b.d.	b.d.	b.d.
Sn	1	b.d.	b.d.	b.d.	b.d.	b.d.	2	2
Tl	b.d.	b.d.	b.d.	b.d.	b.d.	b.d.	b.d.	b.d.
Cs	b.d.	b.d.	b.d.	0.6	0.7	1.2	0.6	0.8
Ga	14	13	11	12	16	12	19	15
Ba	14	23	47	182	1122	100	102	44
Rb	9	8	9	20	45	10	24	20
Sr	114	104	148	116	261	178	89	123
Hf	1.6	1.1	0.9	1.1	1.2	0.5	4.7	1.7
Ta	b.d.	b.d.	b.d.	b.d.	b.d.	b.d.	b.d.	b.d.
Nb	2.2	1.6	b.d.	1.2	3.1	1.2	9.6	2.9
Y	17	14	10	13	12	9	56	22
Zr	56	45	39	37	46	31	167	67
Th	0.2	0.1	b.d.	0.2	0.7	b.d.	0.8	0.2
U	b.d.	b.d.	b.d.	b.d.	0.2	b.d.	0.3	0.2
La	4	3.7	b.d.	3.6	10.1	2.6	11.1	5.1
Ce	8.3	6.5	3.9	5.3	10.8	4.5	30.1	11.1
Pr	1.2	1	0.7	0.8	1.4	0.5	4.7	1.7
Nd	7.1	5.4	3.9	4.3	6.9	3.2	25.9	8.1
Sm	2.1	1.8	1.4	1.5	1.8	0.9	8.2	2.7
Eu	0.81	0.62	0.44	0.61	0.73	0.51	2.38	0.91
Gd	2.9	2.5	2	2.1	2.3	1.6	10.5	3.7
Tb	0.6	0.4	0.3	0.4	0.4	0.2	1.8	0.6
Dy	3.7	2.9	2.3	2.6	2.2	1.7	11.5	4.1
Ho	0.7	0.6	0.5	0.5	0.5	0.4	2.3	0.9
Er	2.2	1.8	1.3	1.6	1.6	1.1	6.9	2.6
Tm	0.31	0.26	0.18	0.23	0.21	0.17	1	0.38
Yb	2.1	1.8	1.3	1.5	1.4	1.3	6.2	2.5
Lu	0.32	0.27	0.24	0.24	0.21	0.13	0.93	0.38
Be	0.3	0.3	b.d.	b.d.	0.3	b.d.	0.9	0.6
As	b.d.	b.d.	b.d.	b.d.	b.d.	b.d.	b.d.	b.d.
Cd	0.3	0.3	0.5	1.4	0.4	0.2	0.2	0.4
Li	8.5	20.5	13.7	28.8	41.3	19.1	9.7	38

Note:
"b.d." refers to analyses below detection; *glom–glomeroporphyritic

bros span a broader range of compositions, from Mg#=23–73, and exhibit similar trends, with the exception that a few samples (both aphyric and glomeroporphyritic gabbronorites) above Mg#~50 show elevated Al_2O_3. The quartz-bearing Menihek gabbros are characterized by the lowest Mg#s (23–55) and the strongest incompatible element enrichment. The Doublet gabbros, including aphyric, glomeroporphyritic, and quartz-bearing gabbronorites, span a more limited compositional range (Mg#=57–69), but appear to follow the same broad trends. The MRD amphibolites span Mg#s=48–62, exhibit the same general trends described above, and fall within the broad compositional ranges defined by the gabbros. For all sample groups, Na_2O (and K_2O; not shown) exhibit significant scatter, likely representing post-magmatic alkali loss.

As noted above, immobile trace elements offer more robust constraints on the primary compositions of altered–metamorphosed igneous rocks owing to their relatively low mobility during alteration and metamorphism. Classification diagrams based on immobile trace elements show that all samples have basaltic compositions and are of predominantly tholeiitic affinity (Figure 6). Figure 7 shows the concentrations of selected trace elements plotted against Zr as the index of fractionation, where higher Zr corresponds to more evolved compositions. Several first-order trends are apparent. For all samples, increasing Zr correlates with an increase in the HFSE (*e.g.*, La, Nb, Th, Y and Yb), and all samples, irrespective of group, fall along the same general trend. The Nb contents of the Le Fer gabbros show a slight scatter. The transition metals (*e.g.*, Cr, Ni) are also somewhat scattered, but in general appear to decrease with increasing Zr. The quartz-bearing Menihek gabbronorites in particular are depleted in these elements.

RARE-EARTH AND MULTI-ELEMENT PATTERNS

Chondrite-normalized REE patterns for the different gabbro groups are shown in Figure 8. For clarity, the diagrams have been restricted to a maximum of 10 representative analyses per group. All samples, irrespective of group, are characterized by overall flat REE patterns, with $(La/Yb)_{CN}$=0.41–2.24. Europium anomalies, calculated as $Eu/Eu^*=(Eu)_{CN}/[(Sm)_{CN}\times(Gd)_{CN}]^{0.5}$, are negligible, ranging from small negative to positive values (Eu/Eu*= 0.73–1.28). The most pronounced negative anomalies (Eu/Eu*=0.73) are exhibited by the quartz-bearing Menihek gabbros. Overall REE abundances (ΣREE) range from ~10–50x chondritic abundances, with the highest values found in the quartz-bearing Menihek gabbros, although this may be an effect of sampling bias. Other important REE ratios (*e.g.*, $(La/Sm)_{CN}$, $(Gd/Yb)_{CN}$, *etc.*) are provided in Table 2.

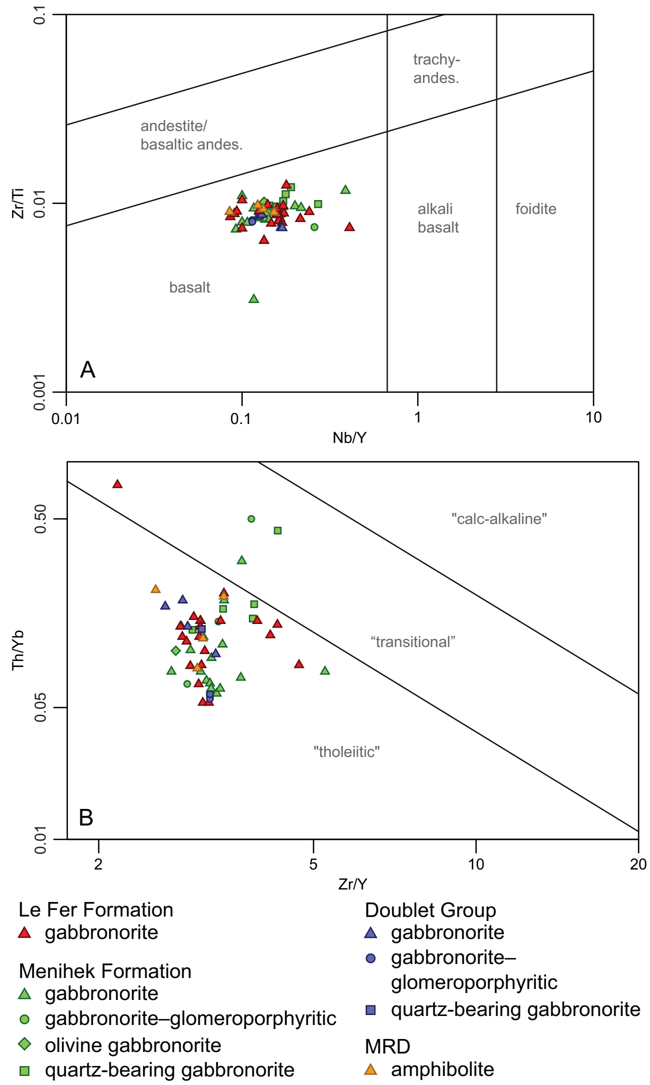

Figure 6. *Immobile trace-element-based classification diagrams. A) Nb/Y* vs. *Zr/Ti diagram of Pearce (1996) showing the basaltic compositions of the analyzed samples; B) Zr/Y* vs. *Th/Yb diagram of Ross and Bedard (2009) showing that the samples are of tholeiitic to transitional affinity.*

Table 2. Selected REE and trace-element ratios (given as ranges) for the different gabbro groups

Group	Doublet (n=8)	Le Fer (n=23)	Menihek (n=34)	MRD (n=4)
$(La/Yb)_{CN}$	0.70–1.51	0.67–1.78	0.41–2.24	0.79–1.69
$(La/Sm)_{CN}$	0.63–1.35	0.60–1.54	0.49–1.88	0.72–1.59
$(Gd/Yb)_{CN}$	1.07–1.17	0.92–1.40	0.92–1.50	1.03–1.71
$(Th/Nb)_{CN}$	0.55–1.10	0.34–7.06	0.28–1.99	0.61–2.60
Eu/Eu*	0.84–1.02	0.76–1.28	0.73–1.23	0.83–1.05
ΣREE	69.2–102.9	66.1–117.4	47.8–237.7	108.6–119.7

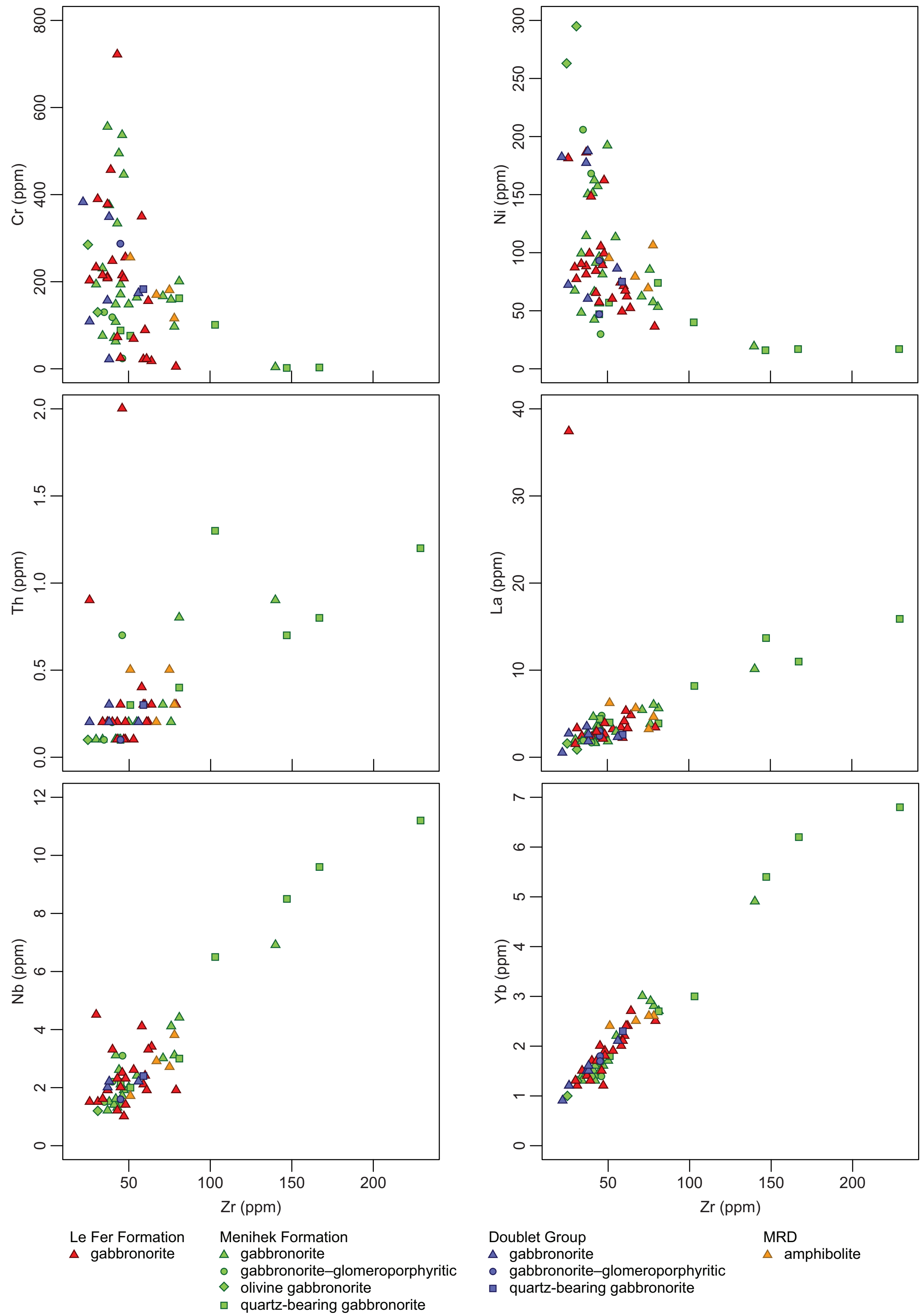

Figure 7. *Bivariate trace-element diagrams showing selected trace elements plotted against Zr.*

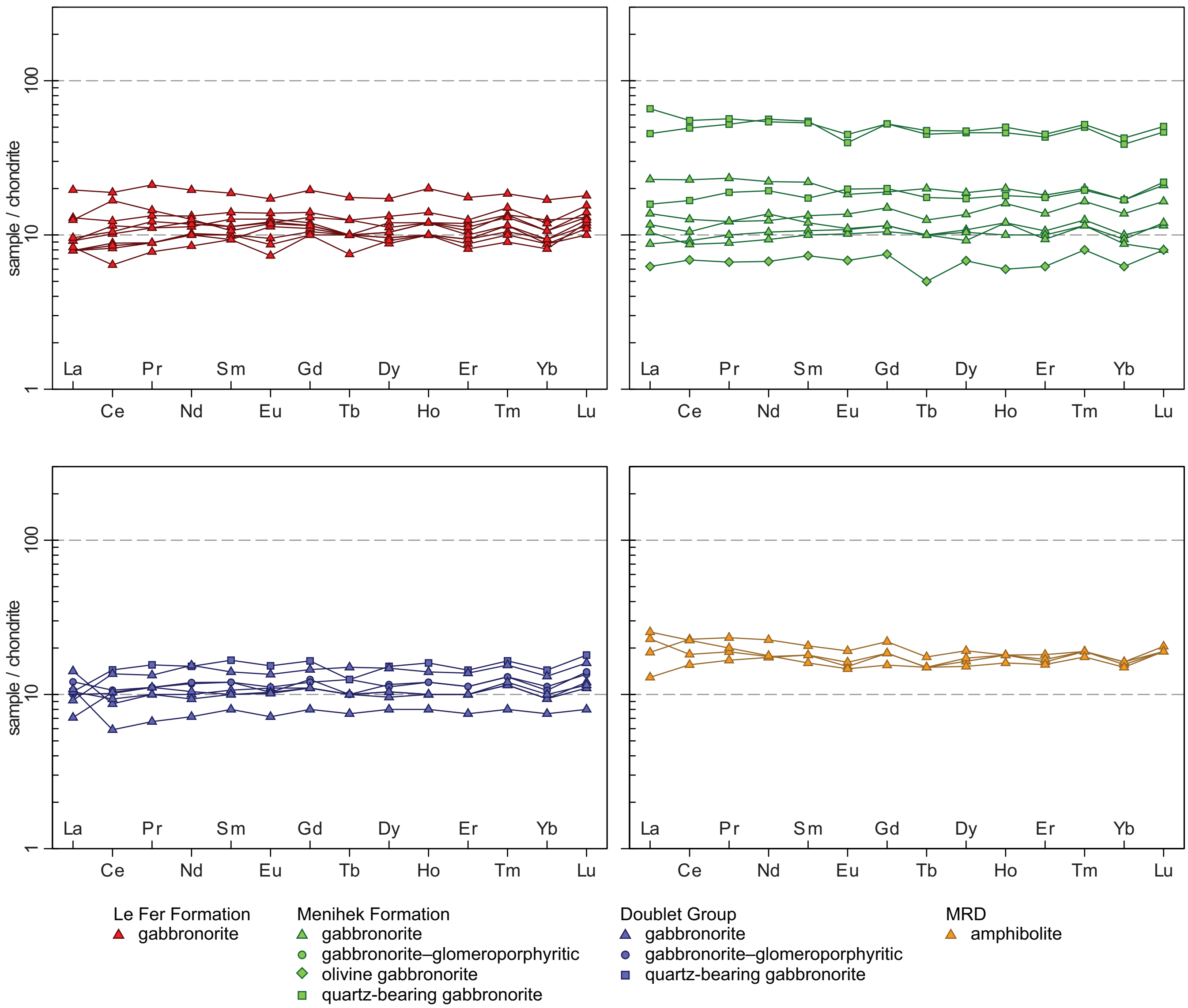

Figure 8. *Chondrite-normalized REE patterns for selected analyzed samples. Normalizing values from McDonough and Sun (1995).*

Primitive mantle-normalized extended trace-element diagrams are shown in Figure 9, along with some average compositions for oceanic basalts (Gale *et al.*, 2013) for comparison. The Le Fer gabbros are characterized by overall flat trace-element patterns (Table 2), with minor troughs at Y. Normalized Th/Nb values are variable, owing to variable Th contents, but are generally low, from $(Th/Nb)_{CN}$=0.34–1.39, with the exception of one sample with $(Th/Nb)_{CN}$=7.06 owing to elevated Th. Many samples contain Th close to, or below the detection limit. Similarly low $(Th/Nb)_{CN}$ is observed for average N-MORB and back-arc-basin basalts (BAB). The Menihek gabbros exhibit similar overall flat trace-element patterns. The most evolved (quartz-bearing) samples show elevated trace-element concentrations and exhibit minor troughs at Ti in addition to Y. The olivine-bearing samples contain lower elemental abundances, in many cases below detection, resulting in irregular patterns with minor to moderate troughs at Hf and Tb. Normalized Th/Nb values range from $(Th/Nb)_{CN}$=0.28–1.99. The Doublet gabbros display patterns similar to the Le Fer gabbros, with relatively flat REE and HFSE, with the exception of minor troughs at Y. Normalized Th/Nb values for the Doublet gabbros range from $(Th/Nb)_{CN}$=0.55–1.10, although several samples contain either Th or Nb below detection. The MRD amphibolites exhibit overall similar trace-element patterns, but show somewhat more variable $(Th/Nb)_{CN}$, from 0.61–2.6.

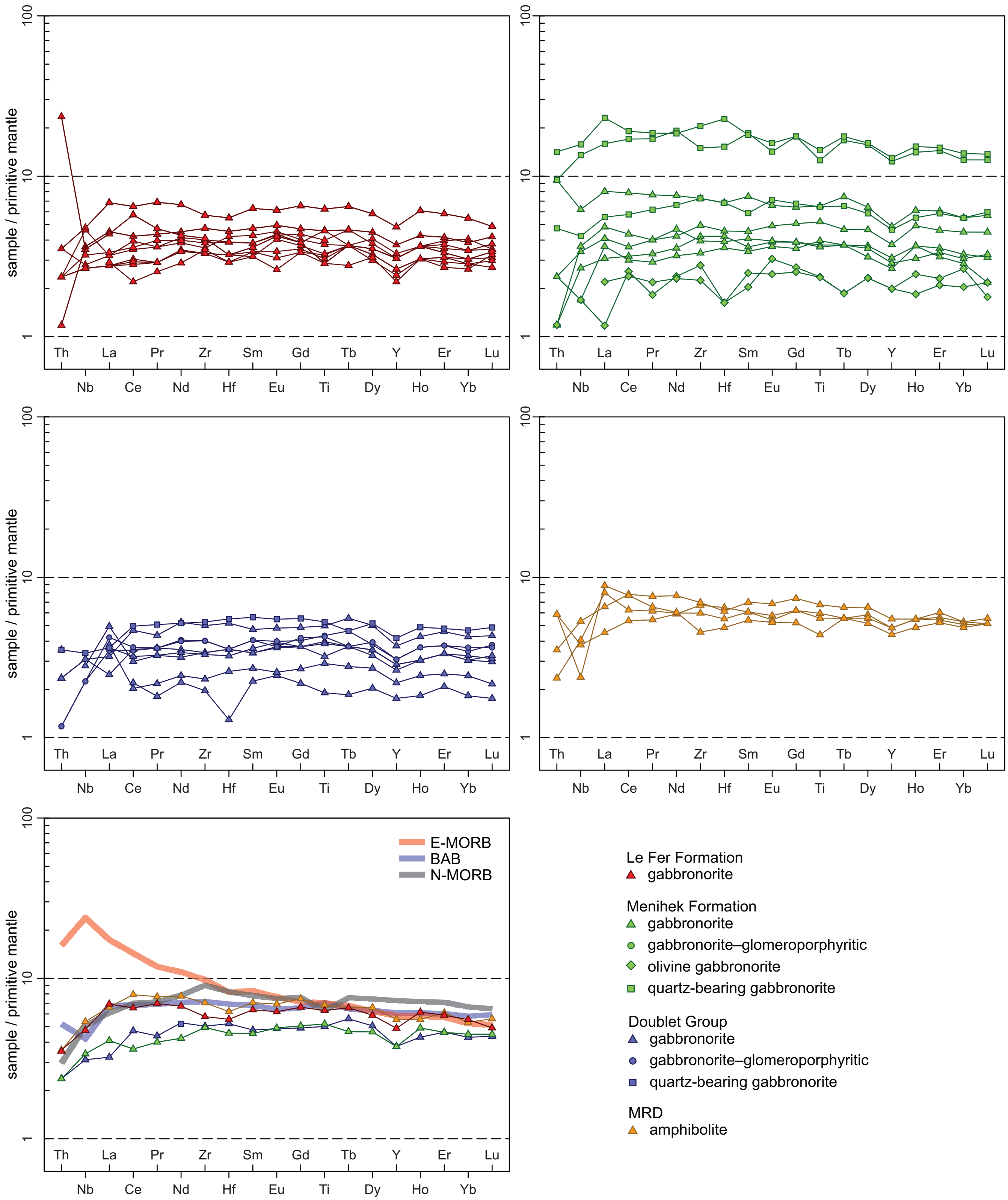

Figure 9. *Primitive-mantle-normalized extended trace-element diagrams for selected samples. Normalizing values from Sun and McDonough (1989). The lower left panel shows selected analyses from each group compared to compositions of average normal and enriched mid-ocean-ridge basalt (N-MORB and E-MORB) and back-arc-basin basalts (BAB) from Gale* et al. *(2013).*

SUMMARY AND PETROGENETIC INTERPRETATION OF GEOCHEMICAL TRENDS

The analyzed samples of the Le Fer, Menihek and Doublet gabbros, and the MRD amphibolites are generally of tholeiitic to weakly transitional basaltic compositions with Mg#s=23–74, and TiO_2 contents from 0.50–3.14 wt. %. The quartz-bearing Menihek gabbros exhibit the most evolved compositions, with Mg#=23, TiO_2=3.14 wt. % and SiO_2=53.66 wt. %, and up to 229 ppm Zr. The sample with the highest Mg# is a Menihek olivine gabbronorite with Mg#=74, TiO_2=0.51, SiO_2=45.88 and 31 ppm Zr.

Major-element compositions of the gabbros fall within similar ranges, with the exception of the quartz-bearing Menihek gabbros, which are significantly more evolved but nonetheless appear to lie along the same trend as the "normal" gabbronorites. In general, the gabbros exhibit decreasing Al_2O_3 and CaO, and increasing SiO_2, TiO_2 and P_2O_5 with increased fractionation (lower Mg#). Bivariate trace-element plots show increasing HFSE with Zr, and generally decreasing Cr, and Ni.

Chondrite-normalized REE patterns of the gabbros are essentially flat, with $(La/Yb)_{CN}$=0.63–2, no significant relative LREE or HREE enrichment ($(La/Sm)_{CN}$=0.49–1.88 and $(Gd/Yb)_{CN}$=0.92–1.71), and negligible Eu anomalies (Eu/Eu*=0.73–1.28). Primitive-mantle-normalized extended trace-element diagrams exhibit relatively flat HFSE and REE patterns within only minor HFSE troughs, and generally low $(Th/Nb)_{CN}$ values (with some exceptions) similar to those of N-MORB or BAB.

The petrogenesis of the Wakuach and Gerido intrusive suites has been examined, in detail, by several authors, most notably Baragar (1960, 1967), and Findlay (1996), although only the latter reported data from the Le Fer (Wakuach Intrusive Suite) gabbros. Readers interested in a detailed examination of sills from the Howse Lake area and further northwest are referred to these sources.

The correlations between certain immobile trace elements exhibited by the gabbros suggest that the observed geochemical variation is the result of fractionation from a compositionally similar parental magma. The observed decreasing Al_2O_3 and CaO with Mg# are consistent with plagioclase fractionation. Similarly, decreasing Ni and Cr with increased Zr are consistent with the fractionation of olivine and clinopyroxene and/or orthopyroxene, respectively. The increases in TiO_2 and P_2O_5 with increased fractionation, meanwhile, suggest that fractionation of ilmenite and apatite were minor. Observations by Findlay (1996) suggest that derivation of the sills from this parental magma was a multistage process involving early fractionation in mid-crustal magma chambers followed by *in-situ* differentiation during emplacement (Findlay, 1996). Early fractionation is evidenced by micro-phenocrysts of the plagioclase, olivine, and pyroxenes within the chilled margins of some Menihek Gabbro sills (Findlay, 1996). Subsequent *in-situ* differentiation was likely the combined result of crystal settling, evidenced in widespread cumulate textures, and flow differentiation, which resulted in the concentration of early formed (resorbed) olivine and plagioclase glomerocrysts in discrete layers within the central parts of sills (Findlay, 1996).

The chondrite-normalized REE and primitive-mantle-normalized extended trace-element diagrams provide further constraints on the petrogenesis of the gabbro sills. The flat, MORB-like REE patterns with negligible Eu anomalies exhibited by all groups are consistent with a relatively high degree of partial melting of a plagioclase-free mantle source. Simple batch-melting calculations following Winter (2001, Table 9–5) show that a similarly flat pattern with $(La/Yb)_{CN}$~1.5 can be achieved by ~25% melting of lherzolite with 60% olivine, 25% orthopyroxene and 15% clinopyroxene, consistent with estimated melting extents of 8–25% for modern ocean-ridge systems (Ahern and Turcotte, 1979; Klein and Langmuir, 1987). Addition of 5% garnet (at the expense of clinopyroxene), meanwhile, raises the melt fraction required to produce $(La/Yb)_{CN}$<1.5 to 60%. The presence of minor Eu anomalies in some samples is likely related to plagioclase fractionation during magma ascent.

Figure 10A show the samples plotted on the Nb/Yb *vs.* Th/Yb diagram of Pearce (2008) and can be used to assess the degree of crustal contamination. Most of the samples plot within the MORB–OIB array (between N-MORB and E-MORB), demonstrating their MORB affinity, and suggesting that they have experienced minimal crustal contamination, with the exception of a few samples that plot above the array. These results are not unlike other basalts erupted on continental margins (*see* Pearce, 2008), for example, the North Atlantic Margin. The Nb/Yb *vs.* TiO_2/Yb diagram (Figure 10B) of Pearce (2008) provides some constraint on the depth of melting, as variations in Ti/Yb can be largely explained in terms of the presence/absence of garnet in the source. Nearly all of the samples plot within the N-MORB field, slightly overlapping E-MORB, and within the MORB array, indicating derivation by shallow mantle melting.

TECTONIC IMPLICATIONS

The Wakuach (Le Fer) and Gerido intrusive suites (Menihek and Doublet) gabbros exhibit very similar major- and trace-element characteristics, despite their dramatically

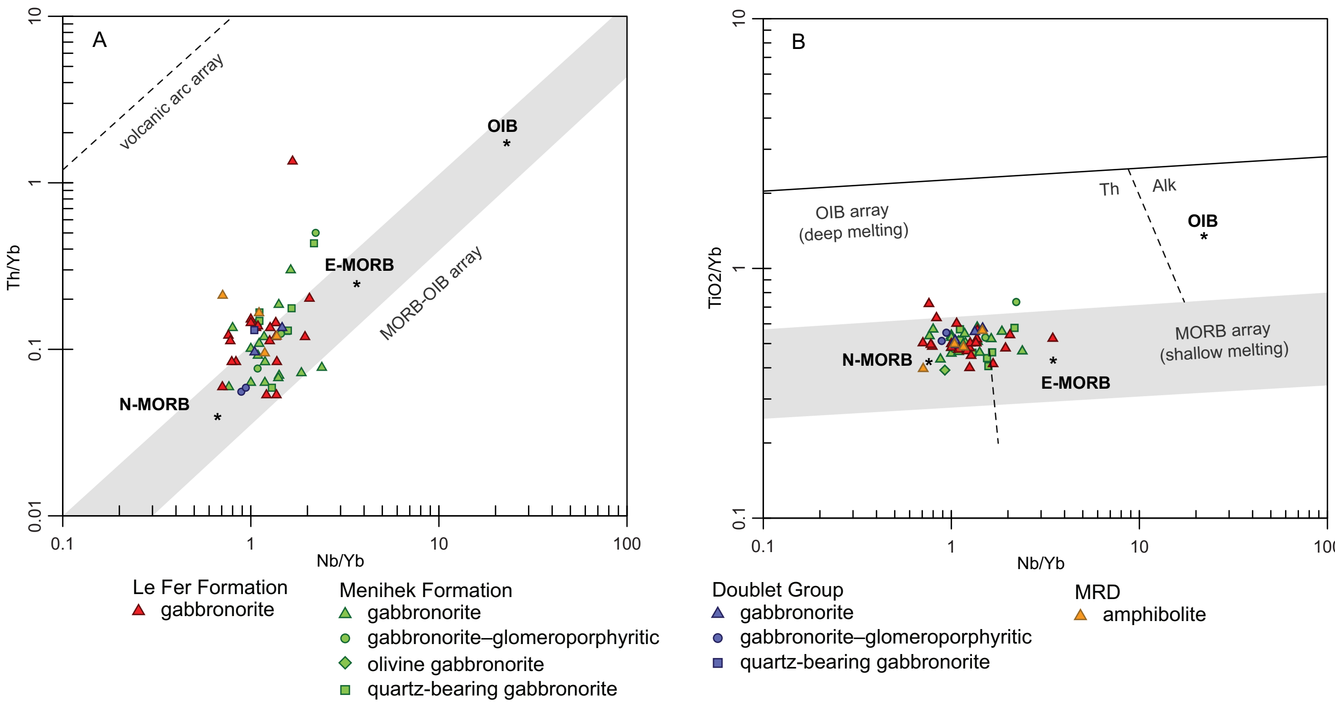

Figure 10. *A) Nb/Yb* vs. *Th/Yb diagram of Pearce (2008) showing samples distributed along the MORB–OIB array, with some samples displaced above the array indicating minor crustal contamination; B) Nb/Yb* vs. *TiO_2/Yb diagram of Pearce (2008), showing samples within the shallow melting array, and one sample in the deep melting array.*

different ages (2.17 *vs.* 1.88 Ga, respectively). The obvious conclusion is that both were derived from compositionally similar magma sources, and probably formed in similar tectonic environments. The present data are generally consistent with previous interpretations that both Cycle 1 and Cycle 2 sill emplacement were the result of multiple stages of lithospheric-scale rifting along the eastern Superior margin (Wardle, 1981; Rohon *et al.*, 1993; Findlay, 1996). Prolonged rifting would have resulted in the development of an ocean basin, presumably to the present-day east of the orogen. However, no ophiolites have been identified in the NQO, and it is possible that the basin in which the KS was deposited remained a narrow embryonic rift throughout much/all of its history (James and Dunning, 2000).

The age of mafic magmatism in the MRD is not known, but the results presented here are compatible with previous inferences that the dykes represent deeper seated equivalents of sills intruded into the KS (Wardle, 1981). James and Dunning (2000) showed that the MRD is probably of Superior affinity, and speculated that it represents a micro-continent-like fragment that was rifted from the Superior margin, possibly during deposition of Cycle 2. The age of MORB-like magmatism in the MRD should offer a potential test for this hypothesis, in that the presence of *ca.* 1.88 Ga ages would imply that the MRD was part of the Superior margin at least until that time.

CONCLUSIONS

Mafic to locally ultramafic sills appear throughout the central NQO, where they form several-km-thick complexes intruded into the volcanosedimentary rocks of the KS. The sills can be divided into two main suites based on their stratigraphic position and presumed age of intrusion. The Wakuach Intrusive Suite gabbros intrude Cycle 1 sediments, and were emplaced *ca.* 2.17 Ga, based on available geochronology. The Gerido Intrusive Suite gabbro (and locally peridotite) sills intruded into Cycle 2 rocks, and were emplaced *ca.* 1.88 Ga. Amphibolites from the MRD have been interpreted as feeder dykes to the sills, although their age is not known.

Most of the examined samples are subophitic gabbronorites. Olivine-bearing samples were observed among the Menihek and Doublet gabbros (representing the Gerido Intrusive Suite). In addition, some Menihek samples contain patchy granophyric quartz–K-feldspar intergrowths. The MRD samples are relatively simple, fine- to medium-grained foliated amphibolites.

All samples, including gabbros of the Wakuach and Gerido intrusive suites, as well as the MRD amphibolites, exhibit broadly similar compositional trends. All are of basaltic composition, and of tholeiitic affinity. Compositional variations among sample groups point to decreasing Al_2O_3 and CaO and increasing SiO_2, with increased fractionation (lower Mg#), and bivariate plots show increasing HFSE with Zr, and generally decreasing Cr, and Ni, features consistent with the fractionation of plagioclase, olivine, clinopyroxene, and orthopyroxene. Rare-earth-element and multi-element diagrams show that the gabbros are all essentially MORB-like, with $(La/Yb)_{CN}$=0.63–2, and negligible Eu anomalies (Eu/Eu*=0.73–1.28).

The present data are consistent with previous tectonic interpretations that sill emplacement was the result of lithospheric-scale rifting of the eastern Superior margin. Available geochronology show that rifting took place in two widely separated stages, although the resulting magmatic products of each are similar. Geochemical similarities suggest the MRD dykes could be co-magmatic with either the Wakuach or Gerido intrusive suite sills, although at present the timing of mafic magmatism in the MRD is not known.

ACKNOWLEDGMENTS

Hamish Sandeman and John Hinchey are thanked for their discussions. Benjamin MacDougall is thanked for his assistance in the field. Oksana Choulik and Wayne Tuttle are thanked for their logistical support. Anne Westhues and Alana Hinchey are thanked for their constructive reviews.

REFERENCES

Ahern, J. and Turcotte, D.L.
1979: Magma migration beneath an ocean ridge. Earth and Planetary Science Letters, Volume 45(1), pages 115-122.

Baragar W.R.A.
1967: Wakuach Lake, Québec–Labrador. Geological Survey of Canada, Memoir 344, 174 pages.

1960: Petrology of basaltic rocks in part of the Labrador Trough. Geological Society of America Bulletin, Volume 71(11), pages 1589-1644.

Bilodeau, C. and Caron-Côté, E.
2018: Géologie de la région de la rivière Arnaud, provinces du Supérieur (Minto) et de Churchill (Fosse du Labrador), secteur de Kangirsuk, Nunavik, Québec, Canada. Ministère de l'Énergie et des Ressources naturelles, Québec, Bulletin Géologique.

Bleeker, W. and Kamo, S.L.
2018: Extent, origin, and deposit-scale controls of the 1883 Ma Circum-Superior large igneous province, northern Manitoba, Ontario, Québec, Nunavut and Labrador. *In* Targeted Geoscience Initiative: 2017 Report of Activities, Volume 2. *Edited by* N. Rogers. Geological Survey of Canada, Open File 8373, pages 5-14.

Butler, J.P.
2019a: Geochemical data from the Montagnais Gabbro sills, Martin Lake rhyolite and associated sedimentary rocks in the Hollinger Lake and Marion Lake areas, Labrador (NTS map areas 23J/16 and 23I/13). Government of Newfoundland and Labrador, Department of Natural Resources, Geological Survey, Open File LAB/1751, 8 pages.

2019b: Geochemical data from supracrustal and basement rocks in the Andre Lake and Marion Lake areas, Labrador (NTS map areas 23I/12 and 13). Government of Newfoundland and Labrador, Department of Natural Resources, Geological Survey, Open File 023I/0103, 8 pages.

2019c: New observations from the Andre Lake area (NTS 23I/12), western Labrador: Tectonic relationships in the hinterland of the New Québec Orogen. *In* Current Research. Government of Newfoundland and Labrador, Department of Natural Resources, Geological Survey, Report 19-1, pages 131-146.

Conliffe, J., Smith, A. and Wilton, D.
2019: Petrographic, geochemical, and sulphur isotope studies of gabbro sills, Labrador Trough: Implications for Ni–Cu–PGE exploration. *In* Current Research. Government of Newfoundland and Labrador, Department of Natural Resources, Geological Survey, Report 19-1, pages 1-21.

Corrigan, D., Wodicka, N., McFarlane, C., Lafrance, I., van Rooyen, D., Bandyayera, D. and Bilodeau, C.
2018: Lithotectonic framework of the Core Zone, southeastern Churchill Province, Canada. Geoscience Canada, Volume 45(1), pages 1-24.

Corrigan, D., Pehrsson, S., Wodicka, N. and De Kemp, E.
2009: The Palaeoproterozoic Trans-Hudson Orogen: A prototype of modern accretionary processes. Geological Society, London, Special Publications, Volume 327(1), pages 457-479.

Clark, T. and Wares, M.
2005: Lithotectonic and metallogenic synthesis of the New Québec Orogen (Labrador Trough). Ministère des Ressources Naturelles, Québec, MM 2005-01, 175 pages.

Clark, T.
1984: Géologie de la région du lac Cambrien, Territoire du Nouveau-Québec. Ministère de l'Ènergie et des Ressources du Québec, ET 83-02, 71 pages.

Finch, C., Roldan, R., Walsh, L., Kelly, J. and Amor, S.
2018: Analytical methods for chemical analysis of geological materials. Government of Newfoundland and Labrador, Department of Natural Resources, Geological Survey, Open File NFLD/3316, 67 pages.

Findlay, J.M.
1996: Petrology, geochemistry and evolution of the Labrador Trough Basaltic Suite, Labrador and New Quebec. Unpublished Ph.D. thesis, University of Ottawa, 612 pages.

Findlay, J.M., Parrish, R.R., Birkett, T.C. and Watanabe, D.H.
1995: U–Pb ages from the Nimish Formation and Montagnais glomeroporphyritic gabbro of the central New Quebec Orogen, Canada. Canadian Journal of Earth Sciences, Volume 32, pages 1208-1220.

Frarey, M.J. and Duffell, S.
1964: Revised stratigraphic nomenclature for the central part of the Labrador Trough. Geological Survey of Canada, Paper 64-25, 13 pages.

Gale, A., Dalton, C.A., Langmuir, C.H., Su, Y. and Schilling, J.G.
2013: The mean composition of ocean ridge basalts. Geochemistry, Geophysics, Geosystems, Volume 14(3), pages 489-518.

Hoffman, P.
1987: Early Proterozoic foredeeps, foredeep magmatism, and Superior-type iron-formations of the Canadian Shield. Proterozoic Lithospheric Evolution, Volume 17, pages 85-98.

1988: United Plates of America, the birth of a Craton: Early Proterozoic assembly and growth of Proto-Laurentia. Annual Reviews of Earth and Planetary Sciences, Volume 16, pages 543-603.

James, D.T. and Dunning, G.R.
2000: U–Pb geochronological constraints for Paleoproterozoic evolution of the Core Zone, southeastern Churchill Province, northeastern Laurentia. Precambrian Research, Volume 103(1-2), pages 31-54.

Klein, E.M. and Langmuir, C.H.
1987: Global correlations of ocean ridge basalt chemistry with axial depth and crustal thickness. Journal of Geophysical Research: Solid Earth, Volume 92(B8), pages 8089-8115.

Lacroix, S. and Darling, R.
1991: Tectonized Cu-Ni deposits of the Aulneau-Redcliff area, central Labrador Trough, Quebec. Economic Geology, Volume 86(4), pages 718-739.

Ludden, J., Gélinas, L. and Trudel, P.
1982: Archean metavolcanics from the Rouyn–Noranda district, Abitibi Greenstone Belt, Quebec. 2. Mobility of trace elements and petrogenetic constraints. Canadian Journal of Earth Sciences, Volume 19(12), pages 2276-2287.

Machado, N., Clark, T., David, J. and Goulet, N.
1997: U–Pb ages for magmatism and deformation in the New Québec Orogen. Canadian Journal of Earth Sciences, Volume 34, pages 716-723.

McDonough, W.F. and Sun, S.S.
1995: The composition of the Earth. Chemical Geology, Volume 120 (#3-4), pages 223-253.

Moorhead, J. and Hynes, A.
1990: Nappes in the internal zone of the northern Labrador Trough: evidence for major early, NW-vergent basement transport. Geoscience Canada, Volume 17, pages 241-244.

Pearce, J.A.
1996: A user's guide to basalt discrimination diagrams. *In* Trace Element Geochemistry of Volcanic Rocks: Applications for Massive Sulphide Exploration. Short Course Notes, Geological Association of Canada, Volume 12, pages 79-113.

2008: Geochemical fingerprinting of oceanic basalts with applications to ophiolite classification and the search for Archean oceanic crust. Lithos, Volume 100, pages 14-48.

Rohon, M.-L., Vialette, Y., Clark, T., Roger, G., Ohnenstetter, D. and Vidal, P.
1993: Aphebian mafic-ultramafic magmatism in the Labrador Trough (New Quebec): Its age and the nature of its mantle source. Canadian Journal of Earth Sciences, Volume 30, pages 1582-1593.

Ross, P.S. and Bedard, J.H.
2009: Magmatic affinity of modern and ancient subalkaline volcanic rocks determined from trace-element discriminant diagrams. Canadian Journal of Earth Sciences, Volume 46, pages 823-839.

Skulski, T., Wares, R.P. and Smith, A.D.
1993: Early Proterozoic (1.88-1.87) tholeiitic magmatism in the New Québec Orogen. Canadian Journal of Earth Sciences, Volume 30, pages 1505-1520.

Smith, A., Conliffe, J. and Wilton, D.
2018: Montagnais Gabbro of western Labrador: Preliminary geological and petrographic data and implications for Ni–Cu–PGE mineralization. *In* Current Research. Government of Newfoundland and Labrador, Department of Natural Resources, Geological Survey, Report 18-1, pages 153-166.

Spitz, G. and Darling, R.
1978: Major and minor element lithogeochemical anomalies surrounding the Louvem copper deposit, Val d'Or, Quebec. Canadian Journal of Earth Sciences, Volume 15(7), pages 1161-1169.

Stauffer, M.R.
1984: Manikewan: an early Proterozoic ocean in central Canada, its igneous history and orogenic closure. Precambrian Research, Volume 25(1-3), pages 257-281.

St-Onge, M.R., Scott, D.J. and Lucas, S.B.
2000: Early partitioning of Quebec: Microcontinent formation in the Paleoproterozoic. Geology, Volume 28(4), pages 323-326.

Sun, S.S. and McDonough, W.F.
1989: Chemical and isotopic systematics of oceanic basalts: implications for mantle composition and processes. Geological Society, London, Special Publications, Volume 42(1), pages 313-345.

Wardle, R.J.
1979: Western margin of the Labrador Trough. *In* Report of Activities for 1978. Government of Newfoundland and Labrador, Department of Mines and Energy, Mineral Development Division, Report 79-1, pages 122-128.

1982: Geology of the south-central Labrador Trough. Government of Newfoundland and Labrador, Department of Mines and Energy, Mineral Development Division, Map 82-005.

Wardle, R.J. and Bailey, D.G.
1981: Early Proterozoic sequences in Labrador. *In* Proterozoic Basins in Canada. *Edited by* F.H.A. Campbell. Geological Survey of Canada, Paper 81-10, pages 331-358.

Wardle, R.J., James, D.T., Scott, D.J. and Hall, J.
2002: The southeastern Churchill Province: synthesis of a Paleoproterozoic transpressional orogen. Canadian Journal of Earth Sciences, Volume 39, pages 639-663.

Wares, R.P. and Goutier, J.
1990: Deformational style in the fore-land of the northern New Quebec Orogen. Geoscience Canada, Volume 17, pages 244-249.

Wilson, A.D.
1960: The micro-determination of ferrous iron in silicate minerals by a volumetric and a colorimetric method. Analyst, Volume 85, Issue 1016, pages 823-827.

Winter, J.D.
2001: An Introduction to Igneous and Metamorphic Petrology. Prentice Hall, 697 pages.